NUCLEAR SCIENCE AND TECHNIQUES **26**, 060103 (2015)

Decommissioning analysis of the scrapers in the NSRL Linac using depth profiling*

HE Li-Juan (何丽娟), LI Yu-Xiong (李裕熊),† LI Wei-Min (李为民), CHEN Yu-Kai (陈裕凯), and REN Guang-Yi (任广益)
National Synchrotron Radiation Laboratory, University of Science and Technology of China, Hefei 230029, China
(Received October 28, 2014; accepted in revised form February 25, 2015; published online December 20, 2015)

For a high-energy electron facility, estimates of induced radioactivity in materials are of considerable importance to ensure that the exposure of personnel and the environment remains as low as reasonably achievable. In addition, accurate predictions of induced radioactivity are essential to the design, operation, and decommissioning of a high-energy electron linear accelerator. In the case of the 200-MeV electron linac of the National Synchrotron Radiation Laboratory (NSRL), the electrons are accelerated by five acceleration tubes and collimated by copper scrapers. The scrapers, which play a vital role in protecting the acceleration cavity, are bombarded by many electrons over a long-term operation, which causes a significant amount of induced radioactivity. Recently, the NSRL Linac is the first high-energy electron linear accelerator in China to be out of commission. Its decommissioning is highly significant for obtaining decommissioning experience. This paper focuses on the measurement of induced radioactivity on the fourth scraper, where the electron energy was 158 MeV. The radionuclides were classified according to their half-lives. Such a classification provides a reliable basis for the formulation of radiation protection and facility decommissioning. To determine the high-radioactivity area and to facilitate the decommissioning process, the slicing method was applied in this study. The specific activity of ^{60}Co in each slice was measured at a cooling time of ten months, and the results were compared with the predictions generated by Monte Carlo program FLUKA. The trend of the measured results is in good agreement with the normalized simulation results. The slicing simulation using Monte Carlo method is useful for the determination of high-radiation areas and proper material handling protocols and, therefore, lays a foundation for the accumulation of decommissioning experience.

Keywords: NSRL Linac, Decommissioning, Scraper, ^{60}Co, Slicing method

DOI: 10.13538/j.1001-8042/nst.26.060103

I. INTRODUCTION

The Synchrotron Radiation Facility of the National Synchrotron Radiation Laboratory (NSRL), located in Hefei, China, is one of the oldest synchrotron light sources in China. The NSRL was home to a 200-MeV electron linear accelerator with a length of 35 m, which served as the injector, and an 800-MeV electron storage ring [1]. Constructed in 1989, the 200-MeV electron linac was a traveling-wave linear accelerator that consisted of five acceleration tubes (in which the electrons are accelerated to 32 MeV, 74 MeV, 116 MeV, 158 MeV and 200 MeV).

The NSRL Linac (Fig. 1) was out of commission in 2012 for a planed upgrade. The induced radioactivity of its components was one of the major concerns of its decommissioning [2, 3]. The NSRL Linac was a large-scale experimental device that was operated for more than twenty years; therefore, it is difficult to provide a detailed historical count of its operation. Figure 2 provides a general historical overview of the NSRL Linac. When accelerated electrons are lost during the operation of such an apparatus, these high-energy electrons will cause electromagnetic cascades when they collided with materials. The resulting high-energy bremsstrahlung will induce photonuclear reactions. Photon activation typically dominates the activation processes that occur in electron accelerators. Furthermore, secondary neutrons produced through photonuclear reactions may contribute to the activation to a certain extent.

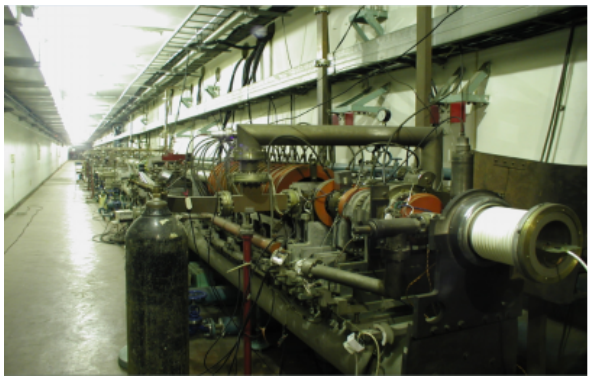

Fig. 1. (Color online) The NSRL Linac.

Residual radioactivity can lead to three radiation safety concerns: personnel exposure, environmental impact, and waste disposal [4, 5]. In a well-shielded accelerator facility, a large portion of the personnel dose result from exposure to radiation from activated components during maintenance work. Additionally, the potential for environmental release of gaseous and liquid radionuclides is a sensitive issue. Furthermore, the disposal of activated materials and the decommissioning of accelerators must be carefully evaluated.

Induced radioactivity may be created in various accelerator components and the surroundings of the accelerator upon direct irradiation by the primary beam or secondary radiation fields [6]. In the NSRL Linac, five copper scrapers were used

* Supported by the National Natural Science Foundation of China (Nos. 11175180 and 11175182)
† Corresponding author, lyx@ustc.edu.cn

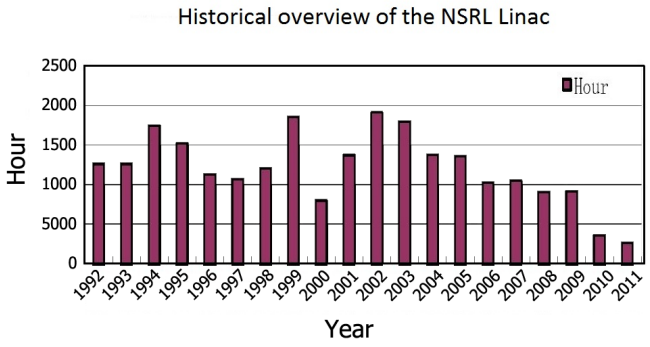

Fig. 2. (Color online) Historical overview of the NSRL Linac operation time.

for beam collimation. The scraper was mounted at the exit of each acceleration tube, and the scraper length increased with increasing electron energies. The scraper aperture had a diameter of 1 cm, smaller than that of the disk-loaded waveguide, which had a diameter of $\emptyset = 2.1997$ cm [7]. Therefore, it is reasonable to assume that electron loss occurred primarily at the scraper during transport and acceleration. Based on this reasoning, the induced radioactivity should have been produced predominantly at the scraper, thereby allowing for easier handling of the structural materials after the retirement of the Linac. The handling of the scrapers was therefore the focus of the decommissioning.

II. MATERIALS AND METHODS

A. Scraper

For the NSRL Linac, to protect the acceleration cavity, each acceleration tube was followed by a scraper. Each scraper was made of copper, and its pore diameter was 1 cm. The pore size of the disk-loaded waveguide was 2.1997 cm. Therefore, the off-center electrons in the beam impacted on the scrapers, creating induced radioactivity.

All the radioactivity of the scrapers originated in electromagnetic cascades and subsequent nuclear reactions. For a 200-MeV electron linear accelerator, the main nuclear reactions are induced by the photons. For copper, the giant resonance threshold is approximately 10 MeV [8, 9]. When a scraper is impacted by a 158-MeV electron beam, the number of photons generated whose energies are within the threshold is the highest. Thus, the induced radioactivity of the fourth scraper is the focus of this paper.

To illustrate the protection of the acceleration tube provided by the scraper, a detailed analysis of the radiation field of the fourth scraper (for an electron energy of 158 MeV) was performed using the latest version of the FLUKA code (version 2011.2). FLUKA is a well-benchmarked, general-purpose tool for calculating particle transport and interactions with matter in a broad range of applications, such as proton and electron accelerator shielding, activation and dosimetry, and radiotherapy [10–12].

Figure 3 illustrates the fourth scraper and the FLUKA simulation model. The size of the scraper is 9.6 cm × 9.0 cm × 3.8 cm (diameter (d) × height (h) × wall thickness (w)). Few electrons should have been lost at the scraper, and the loss position should have been random for every instance of operation at the facility. Based on this reasoning, an annular beam shape (2.2 cm × 0.6 cm ($d \times w$)) and a uniform electron distribution are assumed. As many as 30 000 000 simulations were performed to obtain reliable results. The electron energy spectrum at the end of the scraper and the normalized results for the photon fluence ($E_{\text{photon}} > 9$ MeV) at the fourth scraper are presented in Fig. 4.

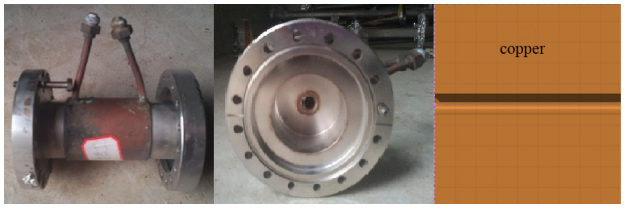

Fig. 3. (Color online) The left image is a photograph of the fourth scraper, and the right image is a top view of the FLUKA model.

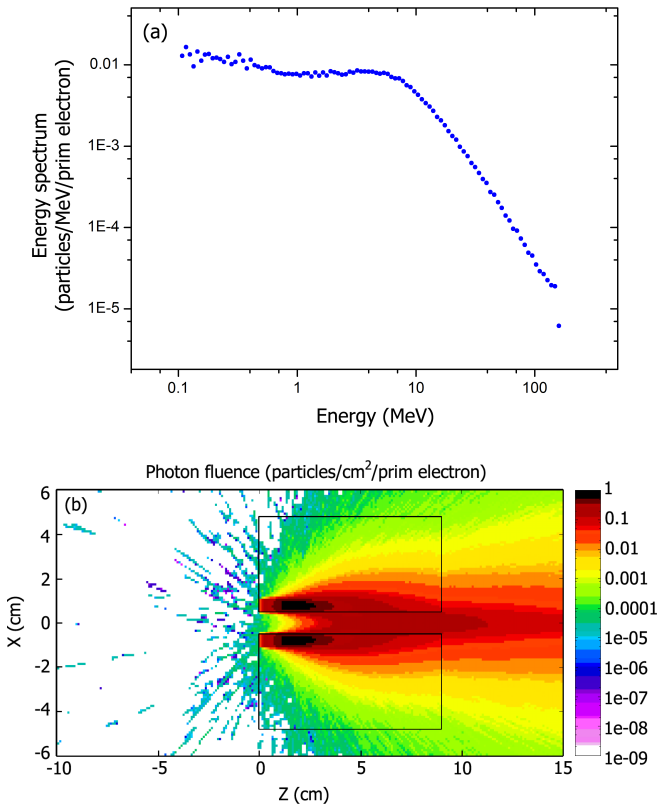

Fig. 4. (Color online) The electron energy spectrum at the end of the scraper (a), and the normalized results for the photon fluence ($E_{\text{photon}} > 9$ MeV) at the fourth scraper (b).

As shown in Fig. 4(a), low-energy electrons at the end of the fourth scraper were dominant and the number of high-

energy electrons was minimal. The majority of the lost electrons were blocked by the fourth scraper. The distribution of photons above 9 MeV is shown in Fig. 4(b), indicating that the most highly concentrated region of photonuclear interaction is in the fourth scraper.

B. Measurement of radioactivity

To investigate the induced radioactivity of the fourth scraper, its γ energy spectrum was measured after the NSRL Linac had been shut down for one hour (5 min "in-beam"). The measuring system consisted of an n-type germanium coaxial detector (portable) (type: GR3519; volume: 31.4426 cm^3; manufacturer: CANBERRA) coupled to an 8000 multichannel analyzer (CANBERRA INSPECTOR 2000). An energy resolution of 1.9 keV and a relative efficiency of 35% at 1332.50 keV were achieved in the system. Energy calibration was performed [13]. The curve of the channel number vs. the γ-ray energy is presented in Fig. 5.

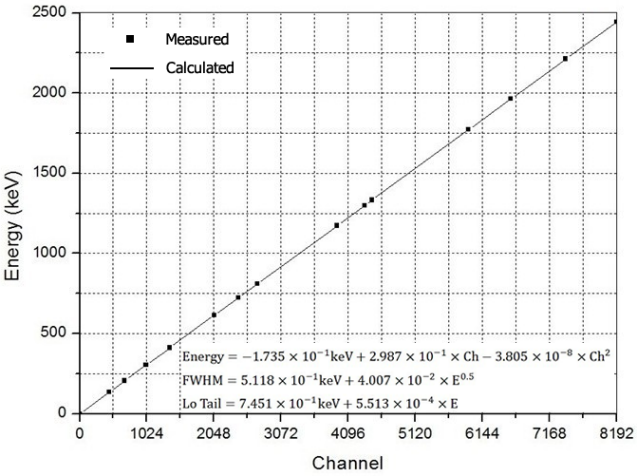

Fig. 5. Energy calibration curve of the high-purity germanium (HPGe) detector (GR3519).

The measurement results of radionuclides in the fourth scraper after 5 min "in-beam" and 1 h "off-beam" are exhibited in Fig. 6. The measured radionuclides were ^{57}Ni, ^{51}Cr, ^{58}Co, ^{56}Co, ^{57}Co, ^{54}Mn, ^{22}Na, and ^{60}Co.

C. Simulation and measurement of ^{60}Co in scraper slices

^{60}Co is the nuclide of greatest importance for the handling of the scraper due to its long half-life ($T_{1/2}$ = 5.27 y). The photonuclear reaction that produces ^{60}Co is ^{63}Cu$(\gamma, n2p)^{60}$Co, and the threshold is 18.86 MeV [8]. The dose rate to the scraper was greater than 10 μGy/h during the initial stage of decommissioning. Once sufficient amounts of radionuclides with short half-lives in a component have decayed, the component can be safely handled. Therefore, we handled the fourth scraper after a cooling time of ten months.

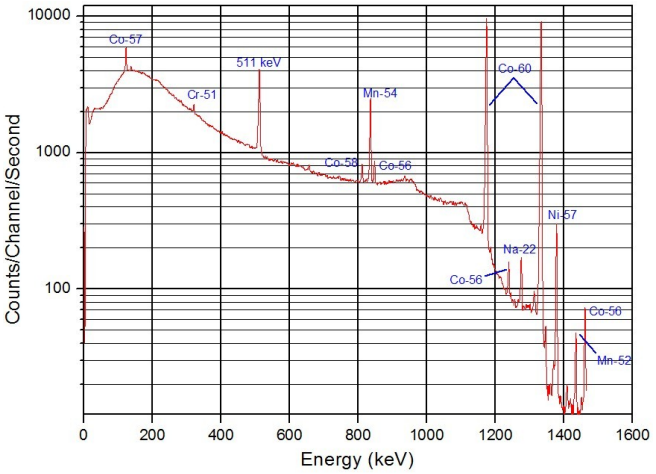

Fig. 6. (Color online) γ-ray spectrum of the fourth scraper.

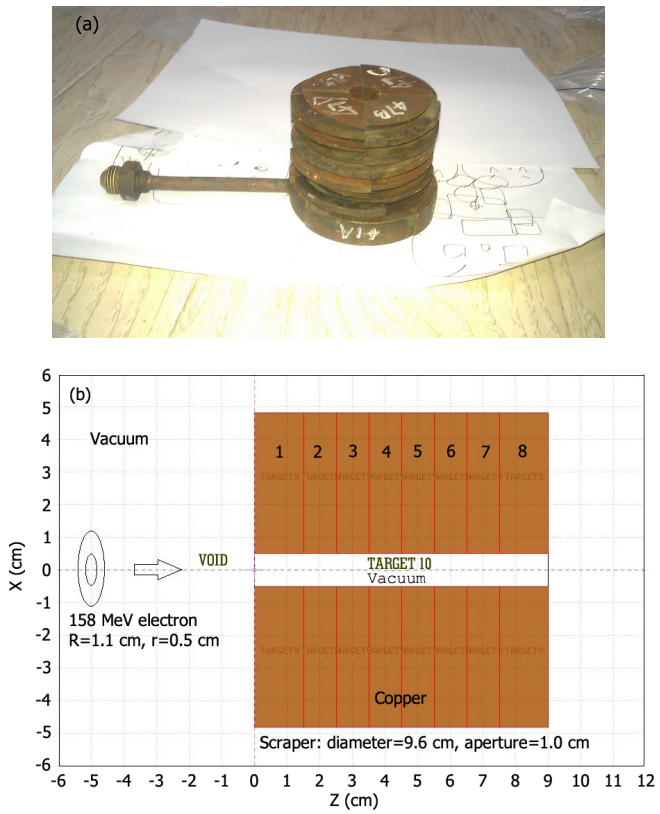

Fig. 7. (Color online) The photograph of the scraper slices (a), and the simulation model (b). The 1st and 8th slices are 1.5 cm in thickness, and the other slices are 1 cm in thickness.

To determine the high-radioactivity area and facilitate the decommissioning process, the slicing method was applied to investigate the ^{60}Co distribution along the axial direction of the scraper. The scraper slices are shown in Fig. 7(a). The first and eighth slices are 1.5 cm in thickness because of the existence of the heat conducting bars. The other slices are 1 cm in thickness. Normalized results for the expected ^{60}Co activ-

ity in the slices were produced using the FLUKA code. The simulation model is depicted in Fig. 7(b).

The concentrations of ^{60}Co in the eight scraper slices after the facility had been shut down for ten months were determined by employing an HPGe γ spectrometer. The employed γ spectrometer (type: GC4019) was a p-type coaxial CANBERRA high-purity germanium detector with a crystal diameter of 62 mm and a thickness of 56 mm. The detector was coupled to a digital multichannel analyzer card system (an 8 k multichannel analyzer, CANBERRA DSA 1000), which, in combination with Genie 2000 software, could be used to determine the area under a peak at a characteristic energy. The HPGe detector was housed inside a massive lead shield consisting of aged lead bricks with a thickness of 10 cm. Such shielding will effectively absorb unwanted radiation from both terrestrial and extraterrestrial sources before it reaches the detector.

Energy calibration of the GC4019 detector was performed. The curve of the channel number vs. the γ-ray energy is presented in Fig. 8. The detector was calibrated using LabSOCS (Laboratory Sourceless Calibration Software, CANBERRA) with a standard precision of less than 10% [14]. During the calibration process, corrections related to self-absorption and solid angle were considered. The dead-time effect was self-corrected by the digital multichannel analyzer. The curve of the γ-ray energy vs. the detector efficiency is presented in Fig. 9 [15]. The energy resolution of the detector was 1.9 keV FWHM at the 1332.50-keV peak of ^{60}Co, and the relative efficiency was 40%. The ^{60}Co activity was evaluated from the photon peak corresponding to its characteristic γ line at 1332.50 keV. Each slice was placed on top of the HPGe detector and counted for a period of 10 000 s. The activity concentrations in the eight scraper slices (specific activities) were measured using the well-known relation given in Eq. (1) [13, 16]:

$$A = \frac{N}{t \times \varepsilon_\gamma \times I_\gamma \times W}, \quad (1)$$

where A is the specific activity in Bq/g, N is the net number of counts in each slice, t is the counting duration, W is the weight of the sample in grams, ε_γ is the detection efficiency at 1332.50 keV, and I_γ is the emission probability of ^{60}Co at 1332.50 keV.

The scraper slices were measured close to the detector in the sample cans. The results of the simulations and the measurements are presented in Fig. 10. The normalized simulation results for the ^{60}Co distribution are in good agreement with the trends observed in the measurements.

III. RESULTS AND DISCUSSION

As shown in Fig. 4, the majority of the lost electrons were blocked by the fourth scraper. The number of high-energy electrons at the end of the fourth scraper was minimal. The results demonstrate that the scraper served as an electron barrier, exerting a protective effect on the acceleration cavity to minimize radiation damage. The FLUKA simulation results indicate that any lost electrons would produce photons. The photon threshold energy for the "giant photonuclear reso-

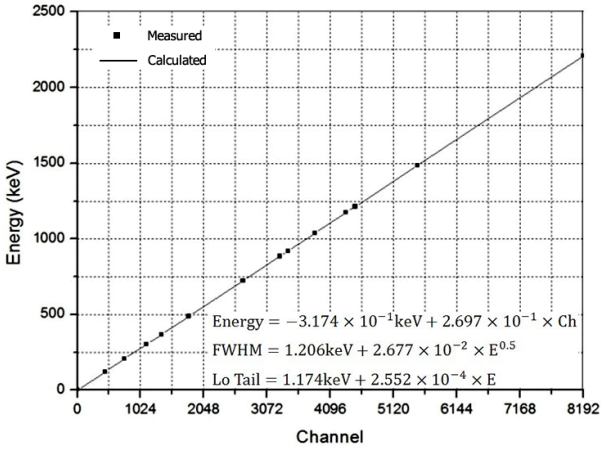

Fig. 8. Energy calibration curve of the HPGe detector (GC4019).

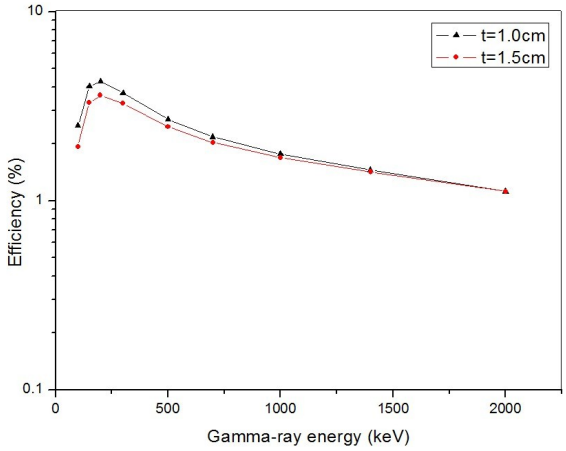

Fig. 9. (Color online) Efficiency curve of the HPGe detector (GC4019) for scraper slices with different thicknesses.

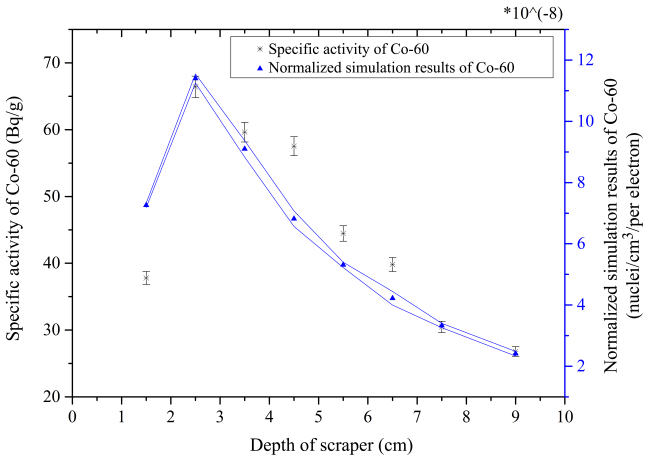

Fig. 10. (Color online) The results of simulations and measurements.

nance" is approximately 10 MeV. The distribution of photons above 9 MeV was calculated, indicating that the most highly concentrated region of photonuclear interaction was expected to be located in the fourth scraper. These results were significant in guiding the handling of the scrapers.

The radionuclides ^{57}Ni ($T_{1/2}$ = 36.0 h), ^{51}Cr ($T_{1/2}$ = 27.72 d), ^{58}Co ($T_{1/2}$ = 71.3 d), ^{56}Co ($T_{1/2}$ = 78.76 d), ^{57}Co ($T_{1/2}$ = 270.9 d), ^{54}Mn ($T_{1/2}$ = 303 d), ^{22}Na ($T_{1/2}$ = 2.602 a), and ^{60}Co ($T_{1/2}$ = 5.263 a) were measured in the fourth scraper after 5 min "in-beam" and 1 h "off-beam". These radionuclides can be classified into three categories according to $T_{1/2}$. First, short-lived nuclides ($T_{1/2}$ on the order of seconds or minutes) are significant to the formulation of radiation protection rules. These nuclides determine the necessary wait time before staff can safely enter the tunnel. Second, the main sources of external radiation exposure for the staff consist of nuclides with $T_{1/2}$ values on the order of hours or days, such as ^{57}Ni. The last category, nuclides with long half-lives, such as ^{54}Mn and ^{60}Co, should be the primary consideration when decommissioning.

The slicing method was applied to determine the distribution of ^{60}Co along the axial direction of the scraper. The normalized simulation results revealed that the region with the highest concentration of ^{60}Co should include the 2nd, 3rd, and 4th slices. The normalized simulation results for the ^{60}Co distribution and the photon fluence are in good agreement with the trends observed in the measurements. These results confirm the reliability of FLUKA simulations. The results indicate that although the 2nd, 3rd and 4th slices represent 1/3 of the volume of the scraper, they contain 50% of the total ^{60}Co in the scraper. These scraper slices were therefore the focus of the scraper handling procedures. According to GB 16487.7-2005 [17], the upper limit on ^{60}Co in non-ferrous metal waste is 0.3 Bq/g. The 2nd scraper slice, with the highest specific activity of ^{60}Co, must therefore be sealed in the waste repository for approximately 29 years.

IV. CONCLUSION

In this paper, we presented simulations of the function of the NSRL scrapers in blocking electrons and protecting acceleration cavity. The scraper design should be carefully considered in the design of electron accelerators and radiation protection. Nuclide classification is critical to the formulation of radiation protection rules and decommissioning. The slicing method combined with FLUKA simulations can be applied to determine the expected nuclide distribution in a scraper along its axial direction. The results of such simulations can assist in determining high-radiation areas, thereby facilitating scraper handling. This method could be extended to the decommissioning of other scrapers corresponding to different electron energies.

ACKNOWLEDGEMENTS

The authors would like to thank the staff of the radiation monitoring stations in Anhui province for their assistance during the measurements.

[1] He D, Pei Y, Jin Y, *et al*. The present status and the future of Hefei National Synchrotron Radiation Light Source. Journal of Shenzhen University Science and Engineering, 1997, **14**: 1–7. (in Chinese)
[2] Sheu R J and Jiang S H. Predicting induced radioactivity for the accelerator operations at the Taiwan Photon Source. Health Phys, 2010, **99**: 788–799. DOI: 10.1097/HP.0b013e3181e84b92
[3] Carbonez P, La Torre F P, Michaud R, *et al*. Residual radioactivity at the CERN 600 MeV synchro-cyclotron. Nucl Instrum Meth A, 2012, **694**: 234–245. DOI: 10.1016/j.nima.2012.08.011
[4] Rokni S H, Fasso A, Gwise T, *et al*. Induced radioactivity of materials by stray radiation fields at an electron accelerator. Nucl Instrum Meth A, 2002, **484**: 680–689. DOI: 10.1016/S0168-9002(01)02064-2
[5] Romanets Y, Bernardes A P, Dorsivaln A, *et al*. Radiation protection, radiation safety and radiation shielding assessment of HIE-ISOLDE. Radiat Prot Dosim, 2013, **155**: 351–363. DOI: 10.1093/rpd/nct005
[6] Smith M, Logar J and Vrain O. Designing a program to assess potential induced radioactivity in electron beam sterilization of medical devices. Radiat Phys Chem, 2014, **105**: 12–16. DOI: 10.1016/j.radphyschem.2014.05.030
[7] Pei Y. Design basis of the electron linear accelerator. Beijing (China): Science Press, 2013.
[8] International Atomic Energy Agency. Radiological safety aspects of the operation of electron linear accelerators. Technical Reports Series No. 188, Vienna, Austria, 1979, 108–114.
[9] Fultz S C, Caldwell J T, Harvey R R, *et al*. Photoneutron cross sections for natural Cu, ^{63}Cu, and ^{65}Cu. Phys Rev B, 1964, **133**: 1149–1154.
[10] Bakkarini F, Battistoni G, Brugger M, *et al*. The Physics of the Fluka Code: Recent Developments. Adv Space Res, 2007, **40**: 1339–1349. DOI: 10.1016/j.asr.2007.05.031
[11] Biju K, Sunil C and Sarkar P K. Estimation of ^{41}Ar production in 0.11 GeV proton accelerator vaults using FLUKA Monte Carlo code. Radiat Prot Dosim, 2013, **157**: 437–441. DOI: 10.1093/rpd/nct148
[12] Qiu R, Liu Y Y, Li W Q, *et al*. Measurement and validation of the cross section in the FLUKA code for the production of ^{63}Zn and ^{65}Zn in Cu targets for low energy proton accelerators. Nucl Sci Tech, 2014, **25**: S010202. DOI: 10.13538/j.1001-8042/nst.25.S010202
[13] Eleftheriou G, Tsabaris C, Androulakaki E G, *et al*. Radioactivity measurements in the aquatic environment using in-situ-laboratory gamma-ray spectrometry. Appl Radiat Isot, 2013, **82**: 286–278. DOI: 10.1016/j.apradiso.2013.08.007
[14] Yang B, Ha Y, Li A, *et al*. Optimisation design of cylindrical containers for improving the detection efficiency of a high-purity germanium detector using the Labsocs. J Radioanal Nucl Chem, 2013, **298**: 1673–1677. DOI: 10.1007/s10967-

013-2577-9
[15] Mohsen B C. Gamma-ray efficiency of a HPGe detector as a function of energy and geometry. Appl Radiat Isot, 2013, **82**: 166–169. DOI: 10.1016/j.apradiso.2013.07.010
[16] Mayeen U K, Panakal J J and Hasan A K. Determination of primordial radionuclides in natural samples using HPGe gamma-ray spectrometry. APCBEE Procedia, 2012, **1**: 187–192. DOI: 10.1016/j.apcbee.2012.03.030
[17] Environmental protection control standard for imported solid wastes as raw materials-Nonferrous metal scraps. GB (China): 16487.7-2005, 28–31.